

## HYDROGEN Ly $\alpha$ AND Ly $\beta$ RADIANCES AND PROFILES IN POLAR CORONAL HOLES

HUI TIAN<sup>1,2</sup>, LUCA TERIACA<sup>2</sup>, WERNER CURDT<sup>2</sup>, AND JEAN-CLAUDE VIAL<sup>3</sup>

<sup>1</sup> School of Earth and Space Sciences, Peking University, 100871 Beijing, China; [tianhui924@gmail.com](mailto:tianhui924@gmail.com)

<sup>2</sup> Max-Planck-Institut für Sonnensystemforschung, 37191 Katlenburg-Lindau, Germany

<sup>3</sup> Institut d'Astrophysique Spatiale, Unité Mixte, CNRS-Université de Paris XI, Bat 121, 91405 Orsay, France

Received 2009 July 5; accepted 2009 September 3; published 2009 September 15

### ABSTRACT

The hydrogen Ly $\alpha$  plays a dominant role in the radiative energy transport in the lower transition region, and is important for the studies of transition-region structure as well as solar wind origin. We investigate the Ly $\alpha$  profiles obtained by the Solar Ultraviolet Measurement of Emitted Radiation spectrograph on the *Solar and Heliospheric Observatory* spacecraft in coronal holes and the quiet Sun. In a subset of these observations, the H I Ly $\beta$ , Si III, and O VI lines were also (quasi-)simultaneously recorded. We find that the distances between the two peaks of Ly $\alpha$  profiles are larger in coronal holes than in the quiet Sun, indicating a larger opacity in coronal holes. This difference might result from the different magnetic structures or the different radiation fields in the two regions. Most of the Ly $\beta$  profiles in the coronal hole have a stronger blue peak, in contrast to those in quiet-Sun regions while in both regions the Ly $\alpha$  profiles are stronger in the blue peak. Although the asymmetries are likely to be produced by differential flows in the solar atmosphere, their detailed formation processes are still unclear. The radiance ratio between Ly $\alpha$  and Ly $\beta$  decreases toward the limb in the coronal hole, which might be due to the different opacity of the two lines. We also find that the radiance distributions of the four lines are set by a combined effect of limb brightening and the different emission level between coronal holes and the quiet Sun.

*Key words:* line: formation – line: profiles – Sun: corona – Sun: transition region – Sun: UV radiation

### 1. INTRODUCTION

As the strongest emission line in the vacuum ultraviolet (VUV) spectral range, the hydrogen Ly $\alpha$  plays a crucial role in the radiative energy transport in the lower transition region (TR; Fontenla et al. 1988). Its radiance and profile provide important information on the structure of the TR, where the solar wind flows out through coronal funnels (Tu et al. 2005; Esser et al. 2005). The solar Ly $\alpha$  line is also very important for interplanetary studies because the spectral irradiance at the center of its profile is the main excitation source responsible for the atomic hydrogen resonant scattering in cool cometary and planetary materials (Emerich et al. 2005).

During the time of *Skylab* (e.g., Nicolas et al. 1976) and the *Orbiting Solar Observatory (OSO 8)*; e.g., Lemaire et al. 1978; Kneer et al. 1981; Vial 1982; Bocchialini & Vial 1996), full Ly $\alpha$  and Ly $\beta$  line profiles were obtained. Ly $\alpha$  spectra in different locations of the Sun were also obtained by the high-resolution telescope and spectrograph (HRTS) instrument on rocket flights (Basri et al. 1979) and by the UVSP instrument onboard the *Solar Maximum Mission (SMM)*; Fontenla et al. 1988). These early observations provided valuable information on the Lyman line profiles. However, since these observations were made in Earth orbits, the obtained Lyman line profiles were hampered by the geocoronal absorption at the center.

The Solar Ultraviolet Measurements of Emitted Radiation (SUMER; Wilhelm et al. 1995; Lemaire et al. 1997) observations at the first Lagrangian point overcame this problem. The whole hydrogen Lyman series is covered by the SUMER spectral range. By analyzing SUMER spectra, Warren et al. (1998) found that the average profiles for Ly $\beta$  through Ly $\epsilon$  ( $n = 5$ ) are self-reversed and show a strong enhancement in the red wings. They also found that the peak separation of these line profiles is larger at limb than at disk center. Xia (2003) found that the asymmetry of the average Ly $\beta$  line profile—the red-peak dominance—is stronger in the quiet Sun than in a coronal hole.

Also in sunspots SUMER observed Lyman line profiles ( $n \geq 2$ ) and Tian et al. (2009b) found that they are almost not reversed, indicating a much smaller opacity above sunspots than in surrounding regions. However, since the Ly $\alpha$  line is so prominent, its high radiance leads to a saturation of the detector microchannel plates. Although attempts were made to observe Ly $\alpha$  on the bare part of the detector, the signal determination was highly uncertain due to the gain-depression correction (Teriaca et al. 2005a, 2005b, 2006).

High-quality Ly $\alpha$  profiles without geocoronal absorption were obtained after 2008 June, when several non-routine observations were made by SUMER. By closing the aperture door to reduce the incoming photon flux to a level of about 20%, the full Ly $\alpha$  profiles were obtained (Curd et al. 2008; Tian et al. 2009a). It turned out that the average Ly $\alpha$  profile in the quiet Sun is strongly reversed and has a stronger blue peak. Moreover, this asymmetry is stronger in regions where the downflows are stronger in the TR.

Here we present new results from these unique data sets. Emphasis is put on the results from a more recent observation in a polar coronal hole region. The different behaviors of Ly $\alpha$  and Ly $\beta$  profiles in the coronal hole as compared to the quiet Sun are presented and discussed. The data set allows for a study of the ratio between Ly $\alpha$  and Ly $\beta$  radiances in the coronal hole. We also investigate the limb brightening effect and the different radiances between coronal holes and the quiet Sun for the two Lyman lines as well as Si III and O VI, by studying their radiance distributions.

### 2. OBSERVATIONS

As mentioned in Curd et al. (2008), we scanned six quiet-Sun regions with a size of  $120'' \times 120''$  at different locations in the equatorial plane on 2008 June 24 and 25. Three regions along the central meridian and including the southern polar region were scanned on 2008 June 26. For these scans, profiles of Ly $\alpha$

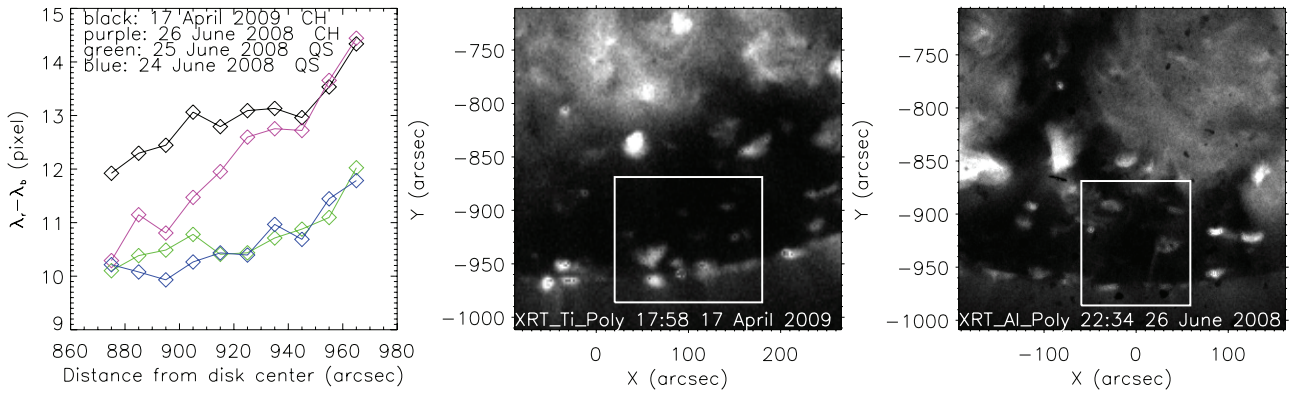


**Figure 1.** Left: the variation of peak separation with the distance from disk center. Middle: XRT image taken at 17:58 on 2009 April 17. Right: XRT image taken at 22:34 on 2008 June 26. In the middle and right panels, the images are displayed in the linear scale; and the white rectangles outline the coronal hole regions scanned by SUMER.

**Table 1**  
Emission Lines Used in this Study

Ion	$\lambda$ (Å)	$\log(T/K)$	Ion	$\lambda$ (Å)	$\log(T/K)$
H I Ly $\alpha$	1215.67	4.0	Si III	1206.51	4.7
H I Ly $\beta$	1025.72	4.0	O VI	1031.93	5.5

**Note.** Here,  $\lambda$  and  $T$  represent the rest wavelength and formation temperature, respectively.

and Si III ( $\lambda$  1206 Å) lines were transmitted to the ground. The scanned region in the southern polar region is outlined in white and is superposed on an X-ray Telescope (XRT; Golub et al. 2007) image, as shown in the right panel of Figure 1. On 2008 September 23, we added a second wavelength setting for Ly $\beta$  and O VI ( $\lambda$  1032 Å) and scanned a quiet-Sun region at the disk center (Tian et al. 2009a). The rest wavelengths and formation temperatures of the four lines are listed in Table 1.

More recently, we adopted these two wavelength settings and scanned a region inside a large coronal hole in the southern polar region from 16:01 to 17:19 on 2009 April 17. Similar to previous observations, we partly closed the aperture door, and could thus reduce the input photon rate by a factor of  $\approx 5$ . As a prologue to the observation, full-detector images in the Lyman continuum around 880 Å were obtained with an open and partially closed door. In this way, accurate values of the photon flux reduction could be established. After this prologue, the slit 7 ( $0'.3 \times 120''$ ) was used to scan the target with a size of about  $150'' \times 120''$ , with an exposure time of 15 s. The scanned region is outlined in white and is superposed on an XRT image, as shown in the middle panel of Figure 1.

The standard procedures for correcting and calibrating the SUMER data were applied, including local-gain correction, dead-time correction, flat-field correction, destretching, and radiometric calibration. Finally, the radiances of the spectra were divided by the factor of the photon flux reduction, which was 18.4% in this observation.

### 3. RESULTS AND DISCUSSIONS

#### 3.1. Peak Separation of Ly $\alpha$

Due to the radiative transfer effect, a central reversal and two peaks in the wings are normally present in Ly $\alpha$  profiles. The peak separation can be regarded as an indicator of the opacity. It has been found that the peak separation is larger at limb

positions than at disk center (Curdt et al. 2008). Here we aim at finding possible differences in the peak separation between coronal holes and quiet-Sun regions at the limb.

We selected four limb scans for this study. For each scan, we first sorted all the data points by the distance from disk center and defined 10 bins. The Ly $\alpha$  profiles in each bin were then averaged to pick up general properties out of the large solar variability. The signal-to-noise ratio is, consequently, very high. By applying a second-order polynomial fit to both peaks of the average profile, we determined the spectral positions of the two peaks  $\lambda_b$  and  $\lambda_r$ . The variations of the peak separation with the distance from disk center are shown in the left panel of Figure 1. The off-disk profiles were excluded in the above calculations since their shapes approximate a Gaussian and show no peaks in the wings.

From Figure 1, we find that in both coronal holes and the quiet Sun the peak separation of the Ly $\alpha$  profile increases toward the limb, indicating a larger opacity combined with a source function decreasing with altitude. This result complements the finding by Warren et al. (1998), in which the authors found that the peak separations of the average profiles for Ly $\beta$  through Ly $\epsilon$  ( $n = 5$ ) are larger at limb than at disk center.

It is also obvious that the peak separation in the polar coronal hole is larger than those in the quiet-Sun region at the east limb. The different behavior of the two coronal holes can be understood if we check the positions of the scans with respect to the coronal hole boundaries. From Figure 1, it is clear that the scanned region on 2009 April 17 was well inside the polar coronal hole. However, the upper part of the scanned region on 2008 June 26 was very close to the boundary, so that the radiance there was likely to be contaminated by the nearby quiet-Sun emission. This effect might explain the fact that the peak separation increases from the quiet-Sun level to the coronal hole level, for the observation on 2008 June 26. Another possibility might be that although coronal radiation is much reduced in the coronal hole (see the following paragraph), from the nearby quiet-Sun structures we may still get quiet a bit of radiation flux which ionizes hydrogen atoms and reduces the opacity. This effect should be weaker with increasing distance from the boundary.

This result indicates a larger opacity in coronal holes, as compared to the quiet Sun. There might be two possible explanations. First, the magnetic field lines in polar coronal holes are almost perpendicular to the line of sight, while they are aligned in various directions at the east limb. It has been shown that since the variations of density and temperature are

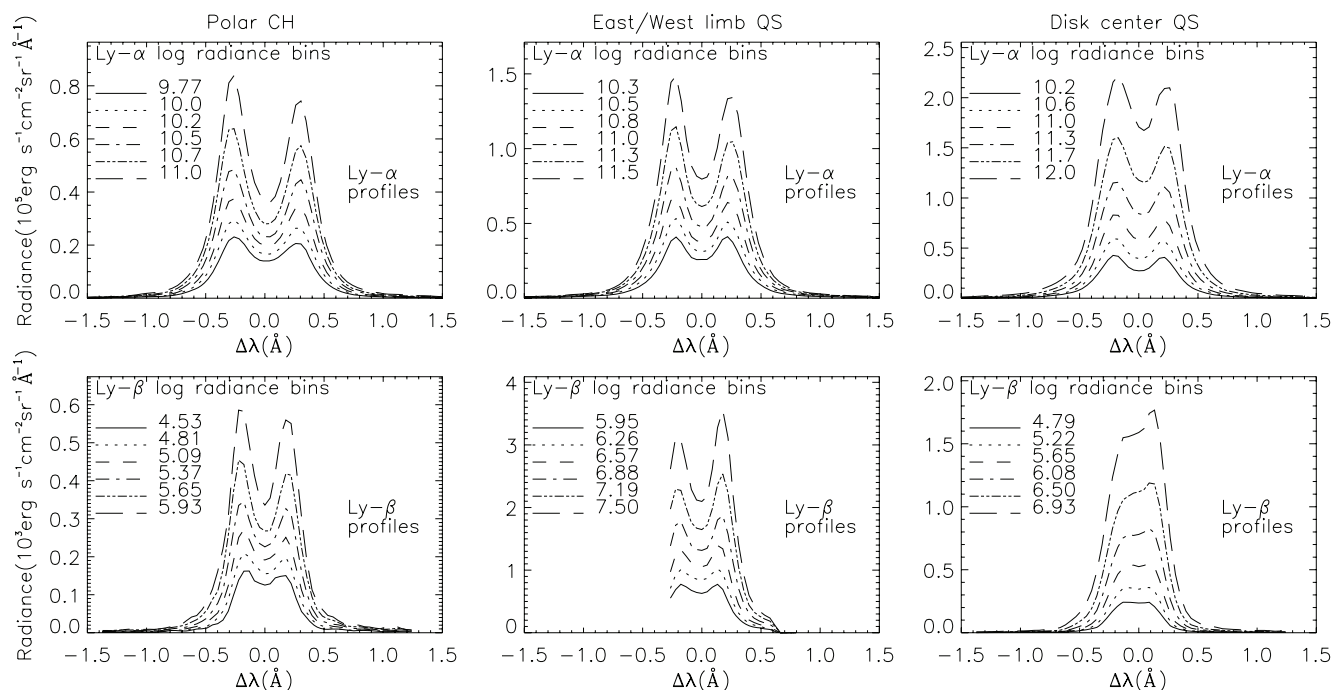


**Figure 2.** Averaged  $\text{Ly}\alpha$  (upper panels) and  $\text{Ly}\beta$  (lower panels) profiles in six different radiance bins, as obtained from a polar coronal hole (left panels, 2009 April 17), a quiet-Sun region at the disk center (right panels, 2008 September 23), and quiet-Sun regions at east limb (upper middle panel, 2008 August 25) and west limb (lower middle panel, 1996 June 7). The level of each bin is also shown in the plots. Here we have excluded spectra acquired off-disk.

different when seen across and along the magnetic field lines, the self-reversal of the Lyman line profiles in a prominence can be different if the prominence is observed from different viewing angles (Heinzl et al. 2005; Schmieder et al. 2007). In coronal holes and quiet-Sun regions, we should not exclude the possibility that the different magnetic structures might influence the  $\text{Ly}\alpha$  profile in the processes of emission and absorption. It is also possible that the larger opacity is the result of a weaker radiation field in the upper atmosphere of coronal holes. Due to the lower radiative ionization, more atomic hydrogen will be populated in the upper TR and corona, which leads to a stronger absorption of the profiles. In order to fully understand this phenomenon, sophisticated models including calculations of non-local thermodynamic equilibrium (non-LTE) radiative transfer should be developed in the future.

### 3.2. Asymmetry of Lyman Line Profiles

Previous observations have shown that the dominant asymmetry for profiles of the hydrogen  $\text{Ly}\alpha$  and higher order Lyman lines is opposite in the quiet Sun. Most  $\text{Ly}\alpha$  profiles have a stronger blue peak (Curdt et al. 2008; Tian et al. 2009a), while most  $\text{Ly}\beta$  profiles have a stronger red peak (Warren et al. 1998; Xia 2003). The asymmetries are probably produced by the combined effects of the differential flows in the solar atmosphere and different line opacities (Gouttebroze et al. 1978; Fontenla et al. 2002; Gunár et al. 2008; Curdt et al. 2008; Tian et al. 2009a).

Similar to Curdt et al. (2008), here we present in Figure 2 the average profiles of  $\text{Ly}\alpha$  and  $\text{Ly}\beta$  in six bins which are equally spaced in radiance. The off-disk profiles were excluded from the averaging. The  $\text{Ly}\beta$  profiles at the west limb were acquired from 13:25 to 14:36 on 1996 June 7, with an exposure time of 10 s. For this observation only 25 spectral pixels were recorded so that the profiles were not complete. Profiles presented in the other five panels are all from the non-routine observations mentioned above. From Figure 2, it is clear that the Lyman line profiles are more reversed at limb positions than at disk center,

which has already been found by Warren et al. (1998) and Curdt et al. (2008).

The most interesting feature in Figure 2 is that the  $\text{Ly}\beta$  profiles in the polar coronal hole have an asymmetry opposite to those in the quiet Sun, while the dominant asymmetry of the  $\text{Ly}\alpha$  profiles is the same in different locations of the Sun. We noticed that Xia (2003) found more locations with blue-peak dominance in  $\text{Ly}\beta$  profiles in equatorial coronal holes than in quiet-Sun regions. However, the average  $\text{Ly}\beta$  profile in Xia (2003) is still stronger in the red peak. Here we find very clearly that most  $\text{Ly}\beta$  profiles are stronger in the blue peak in the polar coronal hole.

Since the asymmetries of the Lyman line profiles are likely to be influenced by flows in various layers of the solar atmosphere, and we know that upflows are predominant in the upper TR and lower corona in coronal holes (Dammasch et al. 1999; Hassler et al. 1999; Tu et al. 2005), it is natural to relate the upflows to the profile asymmetries. In order to investigate this relationship, newly designed observations will be done in the near future. However, the flows of the emitting material might also be different in the coronal hole and quiet Sun, which will also alter the asymmetries of line profiles.

### 3.3. Radiance Ratio between $\text{Ly}\alpha$ and $\text{Ly}\beta$

The  $\text{Ly}\alpha/\text{Ly}\beta$  ratio is very sensitive to the physical and geometrical properties of the fine structures in prominences (Vial et al. 2007). However, this ratio in coronal holes is not well established.

The spectra obtained on 2009 April 17 include both  $\text{Ly}\alpha$  and  $\text{Ly}\beta$  lines, and, thus, allow for studying the center to limb variation of the radiance ratio between  $\text{Ly}\alpha$  and  $\text{Ly}\beta$  in the coronal hole. In Figure 3, we present the radiances of four lines and the ratio  $\text{Ly}\alpha/\text{Ly}\beta$  in 23 bins which are equally spaced in distance. In each bin, the diamond and the vertical bar represent the median value and standard deviation, respectively. The median values and the corresponding standard deviations obtained from the disk-center quiet-Sun region on 2008 September 23 are also

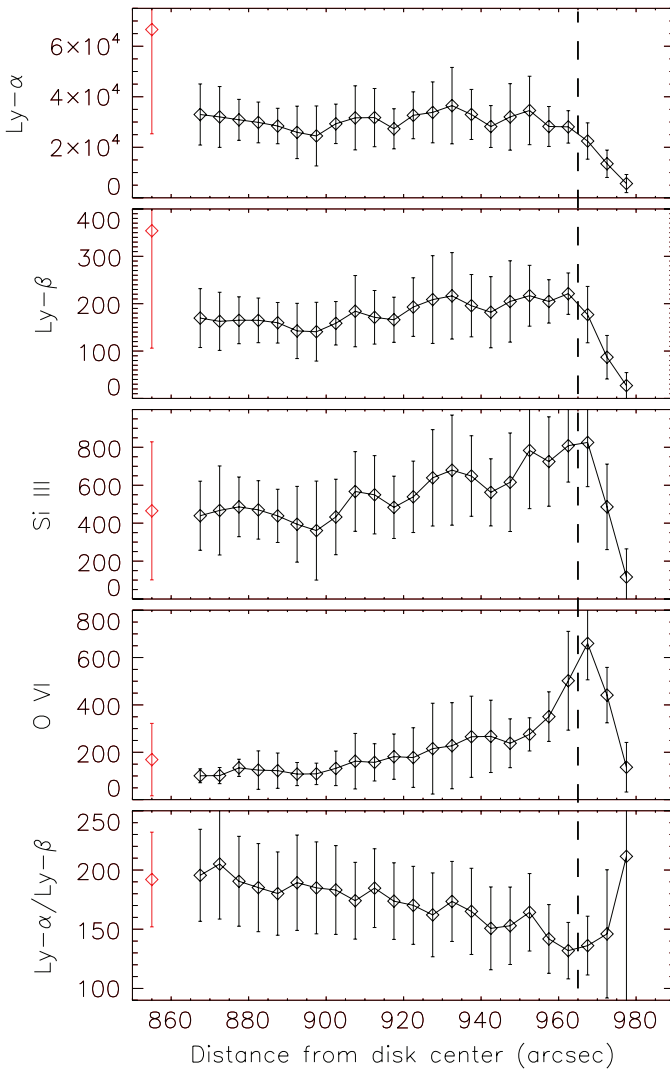


**Figure 3.** Radiances of Ly $\alpha$ , Ly $\beta$ , Si III, and O VI, and the radiance ratio of Ly $\alpha$  and Ly $\beta$ , as obtained from the polar coronal hole on 2009 April 17, are shown as a function of the distance from disk center. In each bin, the diamond and the vertical bar represent the median value and standard deviation, respectively. The median values and the corresponding standard deviations obtained from the disk-center quiet-Sun region on 2008 September 23 are also shown and marked in red for comparison. The unit of the radiance is erg cm $^{-2}$  s $^{-1}$  sr $^{-1}$ . The dashed line indicates the approximate position of the limb.

shown and marked in red for comparison. The radiances are given in energy units of erg cm $^{-2}$  s $^{-1}$  sr $^{-1}$ .

From Figure 3, we can see that the effect of limb brightening is obviously present in the line radiance of O VI, and also clear in Si III. This effect is totally absent in Ly $\alpha$ , which is consistent with Curdt et al. (2008). The effect is present, although not prominent, for Ly $\beta$ . This is because Ly $\beta$  has a smaller opacity and thus should behave more similarly to optically thin lines than Ly $\alpha$ . As a result, the ratio Ly $\alpha$ /Ly $\beta$  decreases toward the limb, from the quiet-Sun level of about 190 to 130 at the limb.

Above the limb, the ratio increases further because the opacity of Ly $\alpha$  stays higher than one, while the lower-than-one Ly $\beta$  opacity leads to a lower radiance. An additional effect might result from the different conditions of formation of the two lines when one goes higher in the atmosphere: the Ly $\alpha$  line becomes scattering dominated (and proportional to the density), while the Ly $\beta$  line stays collision-dominated (and proportional to the square of the density).

### 3.4. Radiance Distribution

Radiance distributions of EUV lines have been intensively studied (e.g., Stucki et al. 2002; Raju & Bromage 2006; Pauluhn & Solanki 2007). Radiance histograms of coronal holes are shifted toward lower values, having a narrower and higher peak indicative of more uniform radiances, as compared to those of quiet-Sun regions. As shown in Raju & Bromage (2006), the radiance distributions are more similar in the quiet-Sun region and the coronal hole for lower-TR lines, while they become increasingly different for lines formed in the upper-TR and corona.

In Figure 4, we present the radiance histograms of Ly $\alpha$ , Ly $\beta$ , Si III, and O VI at different locations of the Sun, by using the spectra obtained in the non-routine observations mentioned above. Again, off-disk data points were excluded from the histograms.

At first sight, the behaviors of the radiance distributions of Si III and O VI are “peculiar.” According to Raju & Bromage (2006), the radiance distribution of the lower-TR line Si III should be similar in coronal holes and in the quiet Sun, and the radiance distribution of the upper-TR line O VI should be shifted toward the weaker side in coronal holes. However, we have to bear in mind that the east-limb region and the polar coronal hole in our study are much closer to the limb, as compared to the polar regions in Raju & Bromage (2006). Thus, the limb brightening effect is much more prominent in our distributions. Due to this effect, the radiance of Si III should be weaker at disk center, and stronger at east/west limb. In polar coronal holes, the radiance should also be stronger than that at disk center, and perhaps slightly weaker than that at east/west limb. This is exactly what we see in the radiance distributions of Si III. For O VI, a combined effect of dark coronal hole emission and limb brightening makes its radiance distribution similar in the polar hole and at disk center. These two effects are clearly revealed by the median of O VI radiances, as shown in Figure 3.

The median values of the radiances shown in Figure 3 also reveal that the polar coronal hole is darker in Ly $\alpha$  and Ly $\beta$ , although these two lines are formed in the lower TR. This behavior is likely due to the large optical thickness. The reduced ionizing coronal radiation may also play a role, as in the case of the He II line (e.g., Raju & Bromage 2006). Since the lines of Ly $\alpha$  and Ly $\beta$  have no or little limb brightening, their radiance distributions in coronal holes are shifted toward the weaker side, as shown in Figure 4.

## 4. SUMMARY

Full hydrogen Ly $\alpha$  profiles which are clean from geocoronal absorption were acquired by SUMER with high spectral and spatial resolutions, through several non-routine observations. In some of these observations, in addition Ly $\beta$ , Si III, and O VI profiles were recorded (quasi-)simultaneously.

The peak separations of Ly $\alpha$  profiles are found to be larger in coronal holes than in the quiet Sun, indicating a larger opacity in coronal holes. This difference might be due to the different magnetic structures or the different radiation fields in the two regions. We also found that the dominant asymmetry of the Ly $\beta$  profiles in the polar coronal hole is opposite to that in the quiet Sun. In order to understand this phenomenon, we need to investigate the influence of the upflows in the upper TR and the flows of the emitting materials on the line profiles. We also investigated the center to limb variation of the radiance ratio between Ly $\alpha$  and Ly $\beta$ , which has a declining trend toward the

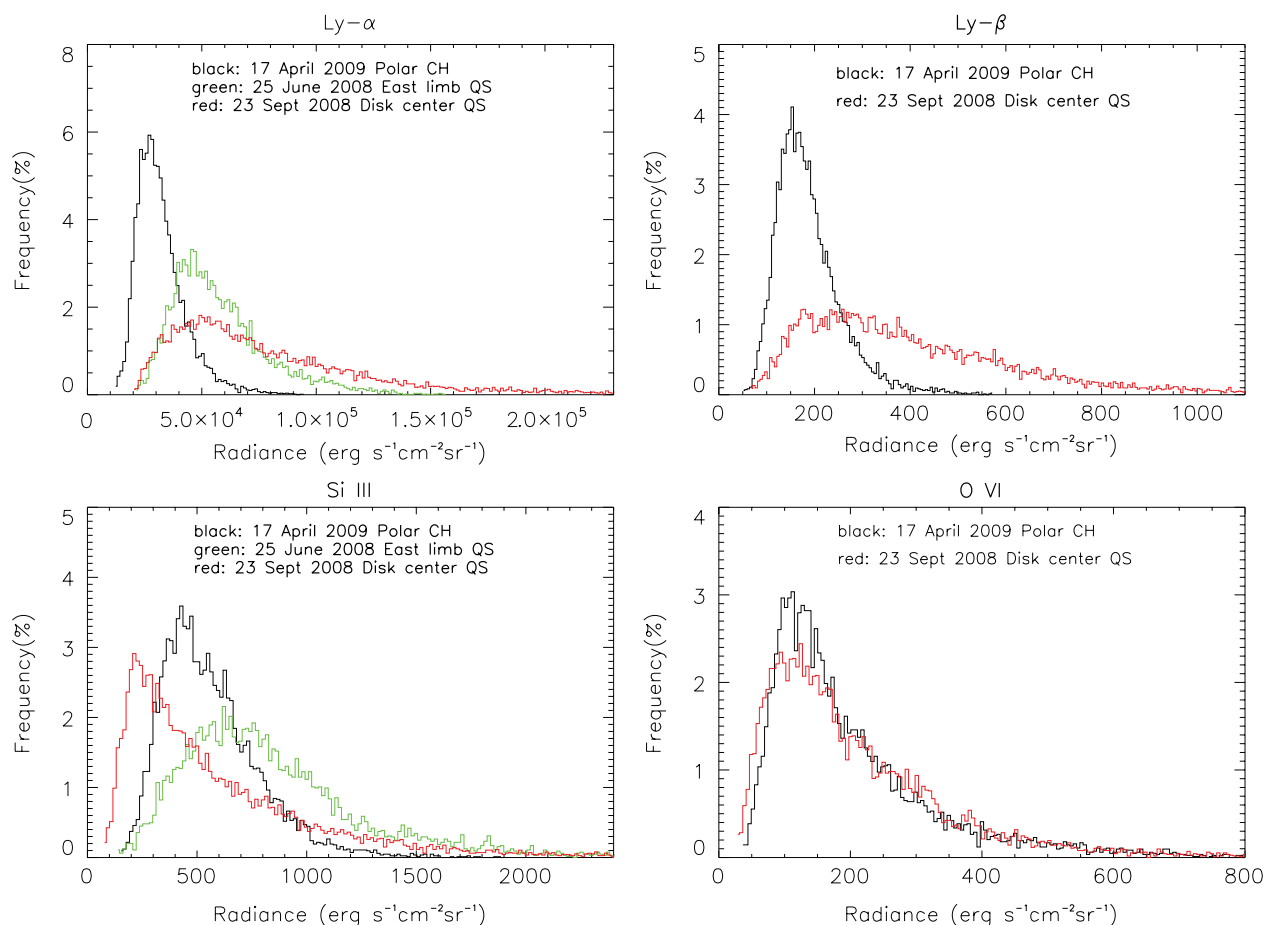


**Figure 4.** Radiance histograms of Ly $\alpha$  (upper left), Ly $\beta$  (upper right), Si III (lower left), and O VI (lower right) at different locations of the Sun. Spectra obtained off-disk were excluded in the analysis.

limb in the coronal hole. Finally, the radiance distributions of the four lines were explained by taking into account the effects of limb brightening and darker emission in coronal holes.

In order to fully understand the above new results, non-LTE models including detailed calculations of radiative transfer should be developed in the future.

SUMER, which is financially supported by DLR, CNES, NASA, and the ESA PRODEX Programme (Swiss contribution), is an instrument onboard *SOHO*. XRT is an instrument onboard *Hinode*, a Japanese mission developed and launched by ISAS/JAXA, with NAOJ as domestic partner and NASA and STFC (UK) as international partners. It is operated by these agencies in cooperation with ESA and NSC (Norway). Hui Tian is supported by the IMPRS graduate school run jointly by the Max Planck Society and the Universities of Göttingen and Braunschweig. The work of Hui Tian's group at Peking University is supported by NSFC under contract 40874090.

## REFERENCES

- Basri, G. S., et al. 1979, *ApJ*, **230**, 924
- Bocchialini, K., & Vial, J.-C. 1996, *Sol. Phys.*, **168**, 37
- Curdt, W., Tian, H., Teriaca, L., Schühle, U., & Lemaire, P. 2008, *A&A*, **492**, L9
- Dammasch, I. E., Wilhelm, K., Curdt, W., & Hassler, D. M. 1999, *A&A*, **346**, 285
- Emerich, C., et al. 2005, *Icarus*, **178**, 429
- Esser, R., Lie-Svendson, Ø., Janse, Å. M., & Killie, M. A. 2005, *ApJ*, **629**, L61
- Fontenla, J. M., Avrett, E. H., & Loeser, E. 2002, *ApJ*, **572**, 636
- Fontenla, J. M., Reichmann, E. J., & Tandberg-Hanssen, E. 1988, *ApJ*, **329**, 464
- Golub, L., et al. 2007, *Sol. Phys.*, **243**, 63
- Gouttebroze, P., Lemaire, P., Vial, J.-C., & Artzner, G. 1978, *ApJ*, **225**, 655
- Gunár, S., Heinzel, P., Anzer, U., & Schmieder, B. 2008, *A&A*, **490**, 307
- Hassler, D. M., et al. 1999, *Science*, **283**, 810
- Heinzel, P., Anzer, U., & Gunár, S. 2005, *A&A*, **442**, 331
- Kneer, F., et al. 1981, *Sol. Phys.*, **69**, 289
- Lemaire, P., et al. 1978, *ApJ*, **223**, L55
- Lemaire, P., et al. 1997, *Sol. Phys.*, **170**, 105
- Nicolas, K. R., Kjeldseth Moe, O., & Tousey, R. 1976, *J. Geophys. Res.*, **81**, 3465
- Pauluhn, A., & Solanki, S. K. 2007, *A&A*, **462**, 311
- Raju, K. P., & Bromage, B. J. I. 2006, *A&A*, **446**, 295
- Schmieder, B., Gunár, S., Heinzel, P., & Anzer, U. 2007, *Sol. Phys.*, **241**, 53
- Stucki, K., et al. 2002, *A&A*, **381**, 653
- Teriaca, L., et al. 2005a, in *ESA SP-596, Proc. Chromospheric and Coronal Magnetic Fields*, ed. D. E. Innes, A. Lagg, & S. K. Solanki (Germany: Katlenburg-Lindau), 66
- Teriaca, L., et al. 2005b, in *ESA SP-600, Proc. ESPM The Dynamic Sun: Challenges for Theory and Observations*, ed. D. Danesy, S. Poedts, A. De Groof, & J. Andries (Belgium: Leuven), 100
- Teriaca, L., et al. 2006, in *ESA SP-617, Proc. 10 years of SOHO and Beyond*, ed. H. Lacoste & L. Ouwehand (Giardini-Naxos, Italy), 77
- Tian, H., Curdt, W., Marsch, E., & Schühle, U. 2009a, *A&A*, **504**, 239
- Tian, H., Curdt, W., Teriaca, L., Landi, E., & Marsch, E. 2009b, *A&A*, in press
- Tu, C.-Y., et al. 2005, *Science*, **308**, 519
- Vial, J.-C. 1982, *ApJ*, **253**, 330
- Vial, J.-C., Ebadi, H., & Ajabshirizadeh, A. 2007, *Sol. Phys.*, **246**, 327
- Warren, H. P., Mariska, J. T., & Wilhelm, K. 1998, *ApJS*, **119**, 105
- Wilhelm, K., et al. 1995, *Sol. Phys.*, **162**, 189
- Xia, L.-D. 2003, PhD thesis (Göttingen: Georg-August-Univ.)